Received: 3 July 2018 | Revised: 21 September 2018 | Accepted: 24 September 2018

DOI: 10.1111/ejh.13179

ORIGINAL ARTICLE

WILEY European Journal of Haematology

Mate pair sequencing improves detection of genomic abnormalities in acute myeloid leukemia

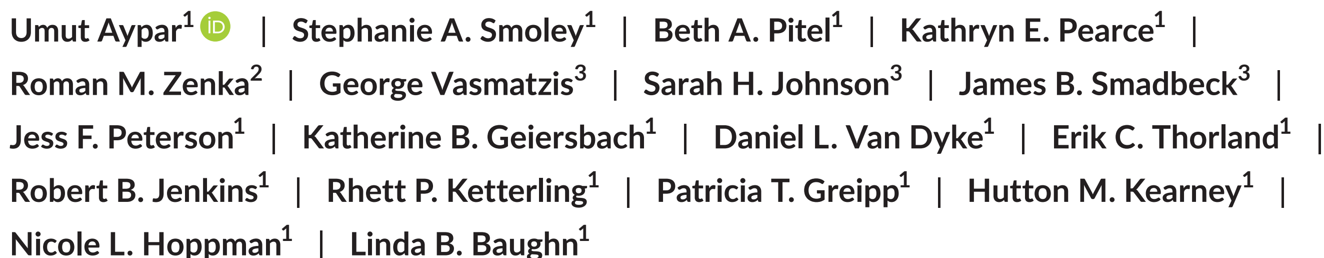

Umut Aypar[1] | Stephanie A. Smoley[1] | Beth A. Pitel[1] | Kathryn E. Pearce[1] | Roman M. Zenka[2] | George Vasmatzis[3] | Sarah H. Johnson[3] | James B. Smadbeck[3] | Jess F. Peterson[1] | Katherine B. Geiersbach[1] | Daniel L. Van Dyke[1] | Erik C. Thorland[1] | Robert B. Jenkins[1] | Rhett P. Ketterling[1] | Patricia T. Greipp[1] | Hutton M. Kearney[1] | Nicole L. Hoppman[1] | Linda B. Baughn[1]

[1]Department of Laboratory Medicine and Pathology, Division of Laboratory Genetics, Mayo Clinic, Rochester, Minnesota

[2]Bioinformatics Systems, Mayo Clinic, Rochester, Minnesota

[3]Center for Individualized Medicine-Biomarker Discovery, Mayo Clinic, Rochester, Minnesota

Correspondence
Linda B. Baughn, Department of Laboratory Medicine and Pathology, Division of Laboratory Genetics, Mayo Clinic, Rochester, MN.
Email: baughn.linda@mayo.edu

Present address
Umut Aypar, Department of Pathology, Memorial Sloan Kettering Cancer Center, New York, New York

Funding information
Mayo Clinic

Abstract

Objective: Acute myeloid leukemia (AML) can be subtyped based on recurrent cytogenetic and molecular genetic abnormalities with diagnostic and prognostic significance. Although cytogenetic characterization classically involves conventional chromosome and/or fluorescence in situ hybridization (FISH) assays, limitations of these techniques include poor resolution and the inability to precisely identify breakpoints.

Method: We evaluated whether an NGS-based methodology that detects structural abnormalities and copy number changes using mate pair sequencing (MPseq) can enhance the diagnostic yield for patients with AML.

Results: Using 68 known abnormal and 20 karyotypically normal AML samples, each recurrent primary AML-specific abnormality previously identified in the abnormal samples was confirmed using MPseq. Importantly, in eight cases with abnormalities that could not be resolved by conventional cytogenetic studies, MPseq was utilized to molecularly define eight recurrent AML-fusion events. In addition, MPseq uncovered two cryptic abnormalities that were missed by conventional cytogenetic studies. Thus, MPseq improved the diagnostic yield in the detection of AML-specific structural rearrangements in 10/88 (11%) of cases analyzed.

Conclusion: Utilization of MPseq represents a precise, molecular-based technique that can be used as an alternative to conventional cytogenetic studies for newly diagnosed AML patients with the potential to revolutionize the diagnosis of hematologic malignancies.

KEYWORDS
acute myeloid leukemia, molecular cytogenetics, MPseq

This is an open access article under the terms of the Creative Commons Attribution-NonCommercial-NoDerivs License, which permits use and distribution in any medium, provided the original work is properly cited, the use is non-commercial and no modifications or adaptations are made.
©2018 The Authors. *European Journal of Haematology* Published by John Wiley & Sons Ltd

1 | INTRODUCTION

Acute myeloid leukemia (AML) is the most common acute leukemia in adults with an incidence of approximately 3-5 cases per 100 000 individuals.[1-3] Approximately 20 000 new cases are diagnosed annually, half of which will die from this disease.[2] The World Health Organization groups AML with recurrent genetic abnormalities into 11 subtypes based on specific chromosomal rearrangements and genetic mutations.[4] An additional category characterized by recurrent cytogenetic abnormalities, including unbalanced copy number variation (CNVs), is defined as "AML with myelodysplasia-related changes".[3] The identification of these well-characterized recurrent genomic abnormalities provides important diagnostic, prognostic, and treatment-related information.

Currently, most genomic testing of bone marrow or blood specimens from AML patients occurs by karyotype analysis, fluorescence in situ hybridization (FISH), or reverse transcription-polymerase chain reaction (RT-PCR) targeting chimeric fusion genes as well as Next-Generation Sequencing (NGS) for the detection of point mutations. While these techniques collectively provide the current gold standard for AML genetic characterization, there are significant limitations including poor and variable resolution of conventional chromosome studies. In addition, cryptic balanced rearrangements may be missed. Karyotyping requires dividing cells arrested in metaphase, is labor-intensive, subjective, requires highly skilled technologists and can result in long turnaround times. While FISH studies address some of these limitations, FISH is limited to the interrogation of only the regions for which FISH probes are available, which requires a priori knowledge of a specific rearrangement or CNV. FISH panels for AML also need to be quite large to be comprehensive. For example, the current Mayo Clinic AML FISH panel contains 29 probe sets (Table S1), and each probe set requires an independent, costly, and time-consuming validation.[5,6] Despite their size, these panels still have the potential to miss cryptic gene fusions resulting from insertional events. While FISH has a higher resolution (100-200 kb compared to >5 Mb) than karyotyping, its resolution is inferior compared to newer methodologies such as chromosomal microarray and NGS technologies, which have the potential to provide more precise characterization of chromosomal abnormalities.

We explored the ability of an NGS methodology, mate pair sequencing (MPseq), to overcome the limitations of conventional karyotyping and FISH studies. MPseq is a whole-genome sequencing assay that utilizes long input DNA (2-5 Kb) that is circularized and fragmented to the size of paired-end fragments (200-500 bp). This modification to traditional NGS sequencing enables the detection of structural rearrangements and copy number changes throughout the genome with significantly reduced sequencing depth, resulting in a more cost-effective strategy. MPseq has higher resolution than karyotyping and FISH, does not require dividing cells or a priori knowledge of specific abnormalities. In addition, MPseq provides an alternative technology to comprehensively evaluate a sample for chromosomal rearrangements and copy number changes in a single assay rather than large panels of independent FISH probes. Here, we compare the performance of MPseq in 68 abnormal and 20 normal samples previously characterized by standard clinical cytogenetic studies to detect chromosome rearrangements and copy number changes in patients with AML. The results described here demonstrate the utility of MPseq as a single assay replacement for conventional karyotyping and FISH studies for diagnostic AML samples and highlight the potential to increase diagnostic yield and clarity.

2 | METHODS

2.1 | Patient samples

All samples were obtained and evaluated as part of an Institutional Review Board approved study. Fresh diagnostic bone marrow (BM), peripheral blood (PB), or fixed cell pellet (FCP) samples from patients with a reason for referral (RFR) of AML referred to the Mayo Clinic Genomics Laboratory were selected based on reported abnormalities previously tested as part of routine clinical care by conventional karyotyping and/or FISH. Due to the scarcity of *BCR/ABL1*-positive AML patients, we included seven patients with CML in order to evaluate *BCR/ABL1* fusions.

2.2 | Conventional chromosome analysis

A conventional G-banded chromosome evaluation was performed as part of routine clinical testing. First, a cell count is performed on the specimen to establish a plating volume and based on the cell count, a corresponding volume of bone marrow is added to two culture flasks containing culture medium and incubated for 24-48 hours at 37°C. In the harvest process, the cells are exposed to colcemid and hypotonic solution, and are fixed with glacial acid and methanol. Metaphase cells are dropped onto microscope slides and are stained by G-banding. All cells analyzed are captured using a computerized imaging system, and one or more karyograms from each clone are prepared to document the type of abnormality and to permit systematic interpretation of the anomalies. Minimal evidence for the presence of an abnormal clone is defined as two or more metaphases with the same structural abnormality or chromosome gain (trisomy), or three or more metaphases lacking the same chromosome. Twenty metaphases are analyzed by qualified clinical cytogenetic technologists and interpreted by a board-certified clinical cytogeneticist.

2.3 | Fluorescence in situ hybridization (FISH)

Commercial and "laboratory-developed" (LD) dual-color dual-fusion (D-FISH), break-apart and enumeration FISH probes were utilized to detect AML-specific abnormalities (Table S1). All specimens were subjected to standard FISH pretreatment, hybridization, and fluorescence microscopy according to specimen-specific protocols. Methods were described in the manuscripts by Aypar et al[5] and Keefe et al.[6] FISH analysis was performed by qualified clinical

cytogenetic technologists and interpreted by a board-certified clinical cytogeneticist.

2.4 | DNA extraction and library preparation

The DNA extraction and mate pair library preparation methods were described in the manuscripts by Johnson et al[7] and Smadbeck et al.[8] Briefly, DNA was isolated from BM and PB samples using the Qiagen Puregene extraction kit when the sample volume was <2 mL, Autopure LS Automated high quality DNA extraction for those samples more than 2 mL, and the QIAmp Tissue kit for fixed cell pellet samples. DNA was processed using the Illumina Nextera Mate Pair library preparation kit and sequenced on the Illumina HiSeq 2500 in rapid run mode. Pooled libraries were hybridized onto a flow cell (two samples per lane) and sequenced using 101-basepair reads and paired-end sequencing.

2.5 | Structural variant bioinformatics pipeline

These and the remaining methods were described in the manuscripts by Johnson et al[7] and Smadbeck et al.[8] MPseq data were processed using BIMA to map to the reference genome and SVAtools for breakpoint detection of both junctions in chromosomal rearrangements and copy number changes (process outlined in Figure 1). BIMA is a binary indexing mapping algorithm for simultaneous mapping of both reads in a mate pair fragment[9] and was used to map all MPseq fragments to reference genome GRCh38 using default settings. BIMA is tuned to detect reads that map to two discontinuous genomic areas, such as when a read crosses a breakpoint or a biotin-junction (common in NGS mate pair library preparation).

Structural variation (SV) was detected by SVAtools, which utilizes the BIMA output to detect and report the breakpoints of structural variants. SVAtools combines three algorithmic approaches: read-pair, split-read, and read depth/count. SVAtools detects junctions of chromosomal rearrangements by clustering the discordant and split-read fragments. Masking and filtering reduce the false-positive clusters to generate a reliable and meaningful list of junctions. Each cluster with at least three fragments, and passing the mask and filter criteria, is called by SVAtools and is considered a putative junction. Copy number variations were detected by SVAtools using the read count of concordant fragments within non-overlapping bins using CNVDetect and Aneuploidy Detection algorithms. CNVDetect uses the list of detected junctions discovered in SVAtools to supplement the edge detection in order to improve resolution and sensitivity. The results from CNVDetect provide calculated normalized read depth (NRD) scores for each region of the genome segmented during the edge detection step. The NRD score estimates the copy number level as compared to the expected normal 2 N copy number level. The Aneuploidy Detection algorithm performs the same calculations used in CNVDetect, but on a chromosome arm level. Instead

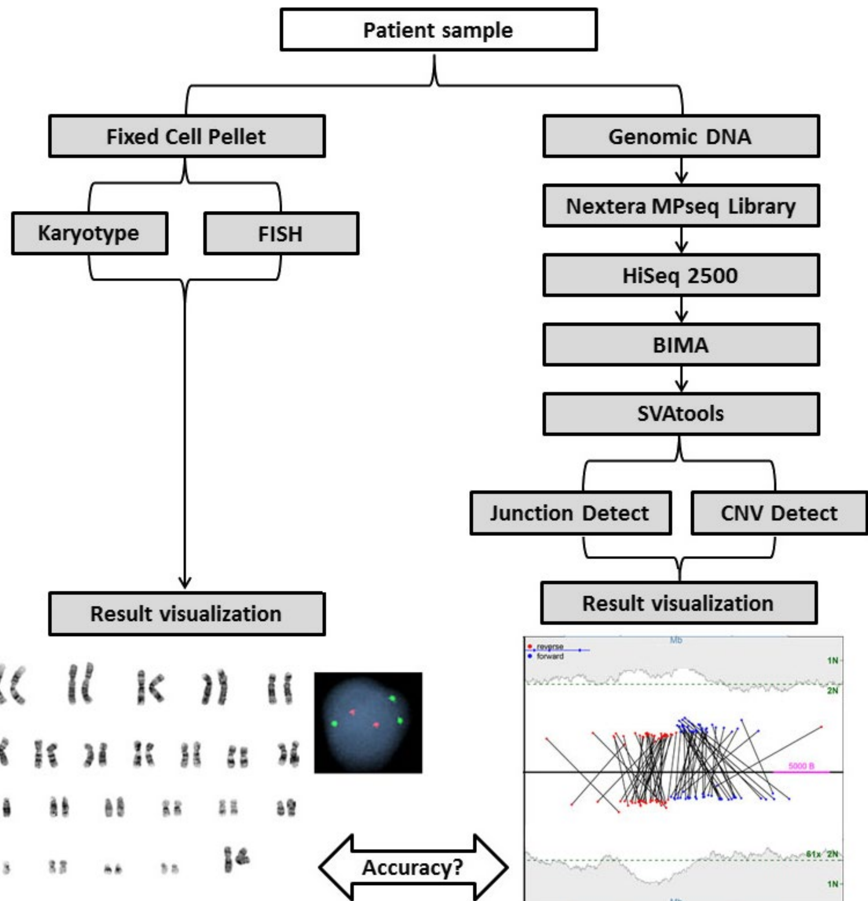

FIGURE 1 Schematic of MPseq AML workflow. Blood or bone marrow samples are processed into fixed cells or extracted for genomic DNA. Fixed cell pellets are processed for karyotype and/or FISH analysis. Genomic DNA is extracted, prepared using the Illumina Nextera Mate Pair library preparation kit and sequenced on a HiSeq 2500. Reads are aligned to the reference genome with BIMA and variants are detected using SVAtools. Two algorithms are utilized for variant detection; junction detection and CNVDetect which also incorporates aneuploidy detection and resulting data are visualized

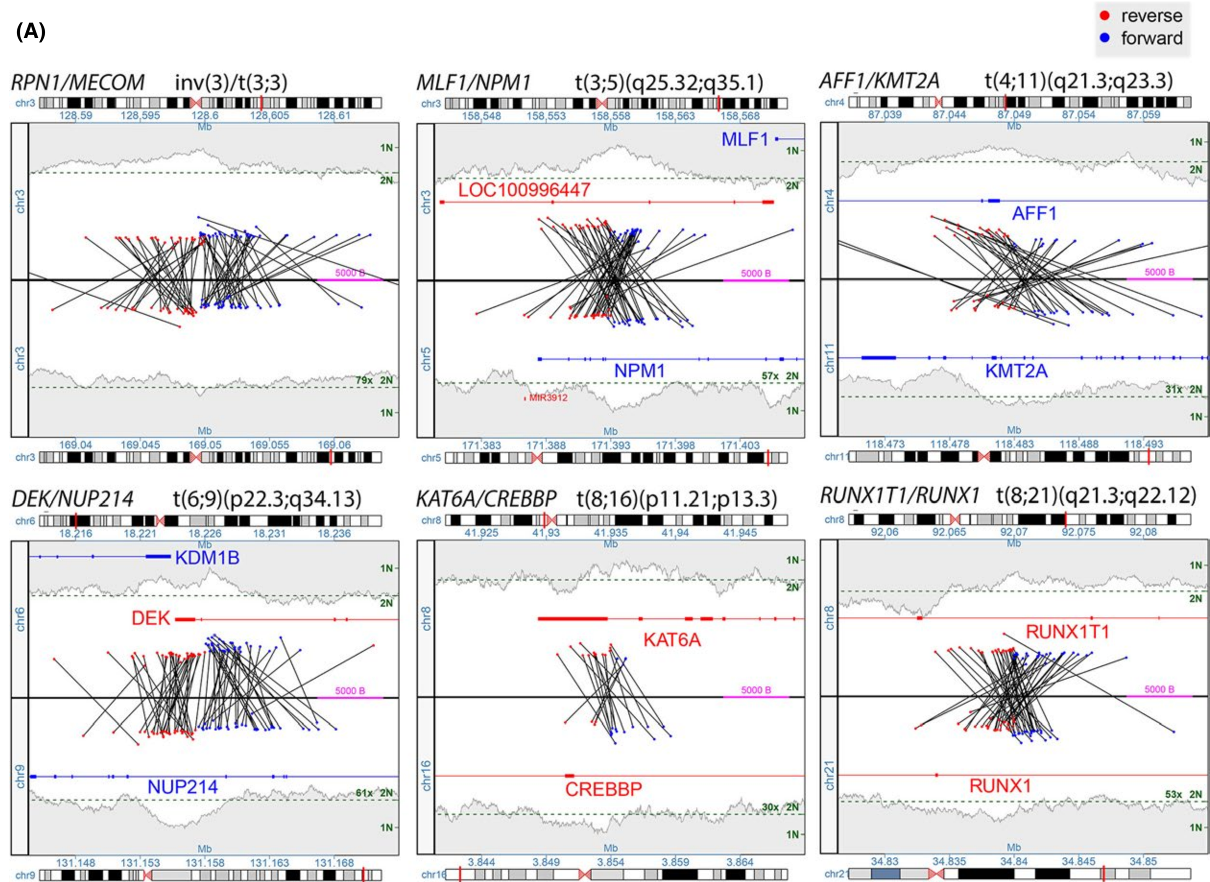
(A)
reverse
forward
RPN1/MECOM inv(3)/t(3;3)
MLF1/NPM1 t(3;5)(q25.32;q35.1)
AFF1/KMT2A t(4;11)(q21.3;q23.3)
MLF1
LOC100996447
NPM1
MIR3912
AFF1
KMT2A
DEK/NUP214 t(6;9)(p22.3;q34.13)
KAT6A/CREBBP t(8;16)(p11.21;p13.3)
RUNX1T1/RUNX1 t(8;21)(q21.3;q22.12)
KDM1B
DEK
NUP214
KAT6A
CREBBP
RUNX1T1
RUNX1
5000 B

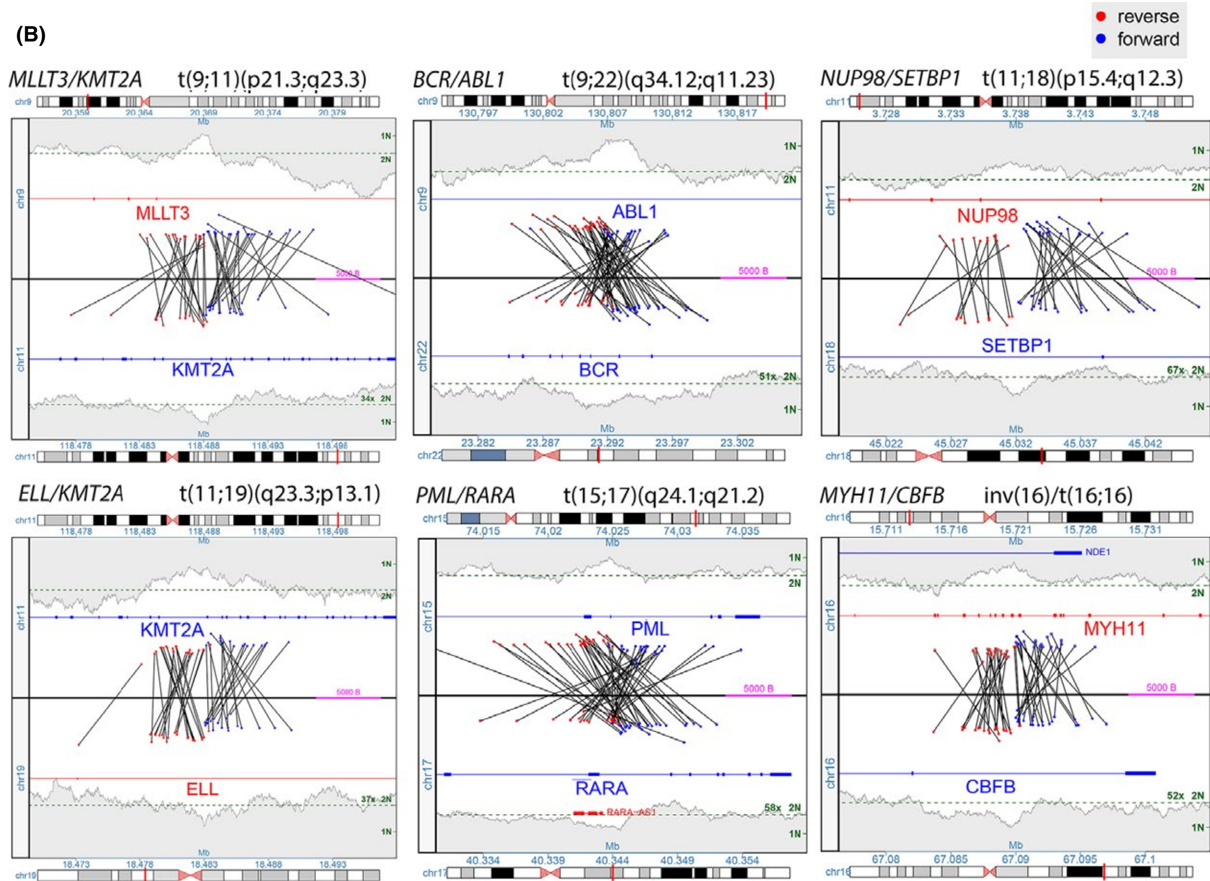
(B)
reverse
forward
MLLT3/KMT2A t(9;11)(p21.3;q23.3)
BCR/ABL1 t(9;22)(q34.12;q11.23)
NUP98/SETBP1 t(11;18)(p15.4;q12.3)
MLLT3
KMT2A
ABL1
BCR
NUP98
SETBP1
ELL/KMT2A t(11;19)(q23.3;p13.1)
PML/RARA t(15;17)(q24.1;q21.2)
MYH11/CBFB inv(16)/t(16;16)
KMT2A
ELL
PML
RARA
RARA-AS1
NDE1
MYH11
CBFB
5000 B

FIGURE 2 (panel A and B) Representative junction plots of the classic-AML rearrangements to be detected by this assay. Each junction plot shows the lowest number chromosome on the top and the higher number on the bottom. Each black line represents a junction between two rearranged fragments with blue in the forward orientation and red in the reverse. Copy state is shown by the gray shaded area on the far top and bottom of the plot. All this data taken together allows for reconstruction of the abnormal region

of segmenting the genome into regions of similar copy number prior to evaluation, each chromosome arm is evaluated as a whole in order to calculate a normalized read depth to compare to the expected 2 N copy number level.

Coverage estimations provide thresholds to confidently call variants. Base coverage (often referred to as depth of coverage, read depth, or coverage) is dependent on the count and length of reads sequenced, and therefore, on total sequenced nucleotides. SVAtools uses a count of the number of fragments spanning a given position, "bridged coverage" to establish confidence for each SV detected. Bridged coverage will depend on the number of fragments and the length the fragments (read lengths plus insert length). Given the bridged coverage of these samples, the reported breakpoints are estimated to be within 200 bps when a split read is not present.[7]

2.6 | Structural variation visualization

Junctions and CNVs were graphically illustrated using genome, junction and region plots as described in Johnson, et al.[7] We restricted our analysis to classic-AML rearrangements involving the genes *ABL1*, *BCR*, *CBFB*, *CREBBP*, *DEK*, *KAT6A*, *MECOM*, *MLF1*, *KMT2A (MLL)*, *MYH11*, *NPM1*, *NUP214*, *NUP98*, *PML*, *RARA*, *RPN1*, *RUNX1*, *RUNX1T1*, and copy number changes on chromosomes 5, 7, 8, 13, 17, and 20 (Figure 2). This restriction was necessary for the validation of the MPseq assay by comparing it to the gold standard FISH assay and FISH probes were available for the above-listed targets. In addition, interstitial CNV regions with no supporting junction, and losses <200 kb and gains <500 kb were not reported. Location of breakpoints identified in each gene from MPseq is indicated along with the specific transcript determined by the consensus transcript from the St. Jude's PeCan Data Portal (Table S3).

3 | RESULTS

To establish the MPseq assay's limits of detection, we evaluated the minimum requirements for (a) DNA input, (b) number of sequenced fragments, and (c) tumor percentage (Supplemental Data, Figures S1-S5 and summarized in Table S2). In summary, eleven samples tested with decreasing amounts of input DNA indicated that the minimum amount yielding accurate results was 0.5 µg (Figure S3). In silico dilution studies of six samples with various rearrangements/CNVs determined that a minimum of 20 million sequenced fragments were required to ensure detection of all targeted abnormalities (Figure S4). Tumor content requirements were assessed by performing various dilutions of six samples with known rearrangements/CNVs, and established a minimum of 10% tumor for the detection of rearrangements and 25% tumor for the detection of CNVs (Figure S5).

3.1 | Detection of primary cytogenetic abnormality using MPseq

We assessed the accuracy of MPseq results compared to results provided by clinical FISH or chromosome studies by evaluating DNA from 68 known abnormal samples extracted from either fresh bone marrow (n = 27), fresh peripheral blood (n = 25) or fixed cell pellets obtained from a conventional chromosome study (n = 16), as well as from 20 karyotypically-normal fresh bone marrow (n = 10) and peripheral blood (n = 10) samples. For all samples, some known variants representing secondary abnormalities as evidenced by FISH studies were present, but below the resolution of the testing performed. The cutoffs of reporting MPseq results were established based on limit of detection data (Supplemental Data, Figures S1-S5 and summarized in Table S2).

All 68 abnormal samples demonstrated concordance with known FISH studies when the abnormal FISH percentage was greater than 10% for rearrangements and greater than 25% for CNVs (Table S2). Three samples (2-PB, 8-BM and 40-BM) were positive for trisomy 8 (each with FISH percentage less than 9%) but were not detected by MPseq (Table 1). Twenty apparently normal samples were also evaluated by MPseq and 19 of 20 were found to be concordant (95%) with no AML-panel abnormalities identified (Table 2).

3.2 | MPseq clarified gene fusions when fish was abnormal

MPseq was necessary to more clearly define the specific gene fusion in eight (12%) of the 68 abnormal cases when FISH either revealed a gene break-apart pattern or three abnormal signals (Table 3). In one of these cases, FISH identified three *BCR* signals when using the *BCR/ABL1* FISH probe (which may indicate *BCR* rearrangement or copy number gain of the *BCR* locus), while MPseq confirmed a *BCR/FGFR1* fusion (1-PB). Similarly, in another case, we identified three *MECOM* signals using the *RPN1/MECOM* FISH probe in the absence of an *RPN1/MECOM* fusion, while MPseq confirmed a *MECOM/CDK6* gene fusion (46-PB). Further, a *TP53/IGL* fusion was found by MPseq in a case with three *TP53* FISH signals (54-BM).

In four cases, MPseq identified the *NUP98* fusion partner (either *PSIP1 or SETBP1* in one case each or *KDM5A* in two cases) when FISH identified a *NUP98* break-apart pattern (no knowledge of the fusion partner). Thus, MPseq was necessary to molecularly define a subset of abnormalities that would not have been elucidated using our current AML FISH panel.

TABLE 1 Accuracy results from 68 known abnormal samples extracted from either fresh bone marrow (n = 27), fresh peripheral blood (n = 25), or fixed cell pellets (n = 16)

		Abnormal Samples n=68																																	
AML Rearrangments		1-PB	2-PB	3-BM	4-BM	5-PB	6-PB	7-PB	8-BM	9-PB	10-BM	11-BM*	12-BM*	13-BM	14-PB	15-BM	16-BM*	17-BM*	18-BM*	19-BM	20-PB	21-BM*	22-BM	23-BM	24-BM*	25-BM*	26-BM*	27-BM*	28-BM	29-PB*	30-BM*	31-PB	32-BM	33-BM	34-PB
BCR/ABL1	t(9;22)(q34.12;q11.23)	68	92	24	15	97	80	51																											
DEK/NUP214	t(6;9)(p22.3;q34.13)								98	94	46																								
KAT6A/CREBBP	t(8;16)(p11.21;p13.3)											57	95																						
AFF1/KMT2A	t(4;11)(q21.3;q23.3)													95	96																				
AFDN/KMT2A	t(6;11)(q27;q23.3)															90	91	95																	
MLLT3/KMT2A	t(9;11)(p21.3;q23.3)																		88	98	99														
MLLT10/KMT2A	t(10;11)(p12.31;q23.3)																					70	95	80											
MLLT1/KMT2A	t(11;19)(q23.3;p13.3)																		84						95	94	97								
ELL/KMT2A	t(11;19)(q23.3;p13.1)																											93	98	96	90				
MLF1/NPM1	t(3;5)(q25.32;q35.1)																															97			
MYH11/CBFB	inv(16)/t(16;16)																																78	90	92
NSD1/NUP98	t(5;11)(q35.3;p15.4)																																		
HOXA9/NUP98	t(7;11)(p15.2;p15.4)																																		
PSIP1/NUP98	t(9;11)(p22.3;p15.4)																																		
NUP98/KDM5A	t(11;12)(p15.4;p13.33)																																		
NUP98/SETBP1	t(11;18)(p15.4;q12.3)																																		
PML/RARA	t(15;17)(q24.1;q21.2)																																		
RPN1/MECOM	inv(3)/t(3;3)																																		
RUNX1T1/RUNX1	t(8;21)(q21.3;q22.12)																																		
Copy Number Variants																																			
-5/5q-		41																																	
-7/7q-																																	38		
Trisomy 8			2						9	8										97								95							
MYC amplification																																			
11q gain																																			
Trisomy 13																						65													
-13/13q-																																			
-17/17p-																																			
TP53 x3																																			
20q-/ider(20q-)																							81												
Trisomy 21																	91									75									

AML Rearrangments		35-PB	36-PB	37-BM	38-BM*	39-BM*	40-BM*	41-BM*	42-BM	43-PB	44-PB	45-BM	46-PB	47-BM	48-PB	49-PB	50-BM	51-BM	52-PB	53-PB	54-BM	55-BM	56-PB	57-BM	58-PB	59-PB	60-BM	61-PB	62-BM	63-BM	64-PB	65-BM	66-BM	67-BM	68-PB
BCR/ABL1	t(9;22)(q34.12;q11.23)																																		
DEK/NUP214	t(6;9)(p22.3;q34.13)																																		
KAT6A/CREBBP	t(8;16)(p11.21;p13.3)																																		
AFF1/KMT2A	t(4;11)(q21.3;q23.3)																																		
AFDN/KMT2A	t(6;11)(q27;q23.3)																																		
MLLT3/KMT2A	t(9;11)(p21.3;q23.3)																																		
MLLT10/KMT2A	t(10;11)(p12.31;q23.3)																																		
MLLT1/KMT2A	t(11;19)(q23.3;p13.3)																																		
ELL/KMT2A	t(11;19)(q23.3;p13.1)																																		
MLF1/NPM1	t(3;5)(q25.32;q35.1)																																		
MYH11/CBFB	inv(16)/t(16;16)	85																																	
NSD1/NUP98	t(5;11)(q35.3;p15.4)		96	89																															
HOXA9/NUP98	t(7;11)(p15.2;p15.4)				99																														
PSIP1/NUP98	t(9;11)(p22.3;p15.4)					74																													
NUP98/KDM5A	t(11;12)(p15.4;p13.33)						26	68																											
NUP98/SETBP1	t(11;18)(p15.4;q12.3)								86																										
PML/RARA	t(15;17)(q24.1;q21.2)									96	85																								
RPN1/MECOM	inv(3)/t(3;3)											80	70																						
RUNX1T1/RUNX1	t(8;21)(q21.3;q22.12)														96	75	83	57	71																
Copy Number Variants																																			
-5/5q-												91								88	71	81	84												
-7/7q-												87	72							90				89	82	94									
Trisomy 8			95				3								54	75				18	64	86													
MYC amplification																											52								
11q gain																												24							
Trisomy 13															67																				
-13/13q-																				87									60						
-17/17p-						94																								62	94				
TP53 x3																					50														
20q-/ider(20q-)																																63	93	95	
Trisomy 21																								45											69

*Sample extracted from a fixed cell pellet; □indicates mate pair provided additional information compared to FISH; ■indicates detected by FISH and mate pair; ■indicates detected by FISH, but not mate pair; ■indicates detected by mate pair, but not tested by FISH. Sample number and type are listed on the *X*-axis, MPseq detected abnormality on the *Y*-axis and percent abnormal by FISH in the corresponding boxes. [Colour table can be viewed at wileyonlinelibrary.com]

3.3 | MPseq detected cryptic rearrangements missed by conventional cytogenetic assays

In two cases, MPseq identified cryptic rearrangements that were not apparent using conventional cytogenetic tests. Sample (78-BM) was initially classified as a normal sample for this verification (Table 2) because we reported a normal karyotype and normal AML FISH panel result. However, the mate pair data specifically demonstrated the insertion of exons 9-24 of *MLLT10* into intron 9 of *KMT2A* resulting from a cryptic, insertional rearrangement which was later confirmed using a *MLLT10/KMT2A* D-FISH probe and not visible by karyotype or by the break-apart *KMT2A* FISH probe (Figure 3 and Table 3). Therefore, this discordance was due to the limitation of the clinical FISH testing approach, as our current clinical AML FISH panel includes the *KMT2A* break-apart FISH probe, and reflex D-FISH *KMT2A* probes are only utilized when there is an abnormal *KMT2A* break-apart result. In another case (47-BM) (Table 3), an apparent t(3;5)(q21;q31) translocation was identified with breakpoints concerning for a *NPM1/MLF1* fusion. MPseq identified a classic *MECOM/RPN1* fusion as part of a more complex 3;5 translocation also involving the *SLC22A5* gene on chromosome 5, and both the *RPN1* locus and *RSRC1* locus on chromosome 3.

4 | DISCUSSION

Here, we describe an NGS-based technology, MPseq, to detect diagnostic and prognostic chromosomal rearrangements and copy number changes in patients with AML. Following an extensive familiarization and pipeline development stage involving >200 samples with detectable cytogenetic rearrangements (data not shown), we tested 88 samples; 68 samples with known recurrent AML rearrangements identified by FISH and/or conventional chromosomes and 20 karyotypically normal samples from patients with a known diagnosis of AML to validate MPseq for AML. When the established minimum limit of detection metrics were achieved (Table S2), the MPseq results from all 88 samples were 98.9% concordant with the existing clinical FISH assay. Importantly, we demonstrate the added clinical value of MPseq, particularly in detecting chromosomal rearrangements that may be cryptic by FISH or when a fusion-specific FISH probe is not available to further characterize an abnormal FISH result. Although these cases were considered concordant by our definition because an abnormality was identified by either FISH or chromosomes, MPseq was necessary to molecularly define the precise gene fusion. This was particularly evident for case 47-BM, which was found to have a t(3;5)(q21;q31) translocation identified by chromosomes concerning for a *NPM1/MLF1* fusion translocation. Because our clinical *NPM1/MLF1* fusion D-FISH probe[5] had not yet been developed, this case was interpreted as having a known, recurrent chromosome abnormality with intermediate prognosis found in various myeloid malignancies particularly MDS/AML.[10] An *NPM1/MLF1* fusion was not identified by MPseq; instead, MPseq revealed a *MECOM/RPN1* fusion associated with aggressive MDS or AML.[10-12] While this case was considered concordant in this validation study, we identified a "cryptic" *MECOM/RPN1* fusion later confirmed by FISH.

MPseq provided further value in cases where we identified additional FISH signals or a FISH break-apart result without the availability of a reflex FISH probe to further define a suspected rearrangement. One example (case 1-PB) is the identification of an

TABLE 2 Accuracy results from 20 karyotypically normal fresh bone marrow (n = 10) and peripheral blood (n = 10) samples [Colour table can be viewed at wileyonlinelibrary.com]

AML Rearrangments		69-BM	70-BM	71-BM	72-BM	73-BM	74-BM	75-BM	76-BM	77-BM	78-BM	79-PB	80-PB	81-PB	82-PB	83-PB	84-PB	85-PB	86-PB	87-PB	88-PB
BCR/ABL1	t(9;22)(q34.12;q11.23)																				
DEK/NUP214	t(6;9)(p22.3;q34.13)																				
KAT6A/CREBBP	t(8;16)(p11.21;p13.3)																				
AFF1/KMT2A	t(4;11)(q21.3;q23.3)																				
AFDN/KMT2A	t(6;11)(q27;q23.3)																				
MLLT3/KMT2A	t(9;11)(p21.3;q23.3)																				
MLLT10/KMT2A	t(10;11)(p12.31;q23.3)										92										
MLLT1/KMT2A	t(11;19)(q23.3;p13.3)																				
ELL/KMT2A	t(11;19)(q23.3;p13.1)																				
MLF1/NPM1	t(3;5)(q25.32;q35.1)																				
MYH11/CBFB	inv(16)/t(16;16)																				
NSD1/NUP98	t(5;11)(q35.3;p15.4)																				
HOXA9/NUP98	t(7;11)(p15.2;p15.4)																				
PSIP1/NUP98	t(9;11)(p22.3;p15.4)																				
NUP98/KDM5A	t(11;12)(p15.4;p13.33)																				
NUP98/SETBP1	t(11;18)(p15.4;q12.3)																				
PML/RARA	t(15;17)(q24.1;q21.2)																				
RPN1/MECOM	inv(3)/t(3;3)																				
RUNX1T1/RUNX1	t(8;21)(q21.3;q22.12)																				
Copy Number Variants																					
-5/5q-																					
-7/7q-																					
Trisomy 8																					
MYC amplification																					
11q gain																					
Trisomy 13																					
-13/13q-																					
-17/17p-																					
20q-/ider(20q-)																					
Trisomy 21																					

■ indicates detected by mate pair, but not by FISH. Sample number and type are listed on the *X*-axis, MPseq detected abnormality on the *Y*-axis and percent abnormal by FISH in the corresponding boxes.

TABLE 3 Additional information obtained from MPseq testing on nine samples that were not apparent through conventional karyotyping or FISH studies

	Additional information from MPseq	Abnormal FISH pattern	Karyotype
1-PB	identified the BCR partner as FGFR1	(BCR)x3[341/500]	BM - 46,XX,t(8;22)(p11.2;q11.2)[3]
39-BM[a]	identified the NUP98 partner as PSIP1	(NUP98x2)(5'NUP98 sep 3'NUP98x1)[148/200]	45,XX,add(1)(p22),add(2)(p13),der(4)t(1;4)(p32;q21),-5,inv(6)(p11.2q21),t(9;11)(p22;p15),-12,add(12)(p13),add(15)(p15),add(16)(q22),add(17)(p11.2),add(20)(p13),+mar[cp20]
40-BM[a]	identified the NUP98 partner as KDM5A	(NUP98x2)(3'NUP98 con 5'NUP98x1)[51/100]	46,XY,del(13)(q12q22)[2]/48,idem,+6,+8[1]/46,XY[17]
41-BM[a]	identified the NUP98 partner as KDM5A	(NUP98x2)(3'NUP98 sep 5'NUP98x1)[135/200]	46,XX,+6,dic(14;19)(p13;p13.3)[14]/48,X,t(X;7)(q24;q11.2),+6,+7[5]/48,sl2,del(13)(q12q22)[1]
42-BM	identified the NUP98 partner as SETBP1	(NUP98x2)(3'NUP98 con 5'NUP98x1)[171/200]	46,XX,del(5)(q31q33),add(11)(p15),add(18)(q21)[16]/46,sl,add(6)(q21)[2]/46,XX[2]
46-PB	identified the MECOM partner as CDK6	(RPN1x2,M ECOMx3)[348/500]	BM - 46,XX,del(7)(q22q34)[6]
47-BM	identified a complex MLF1/MECOM/RPN1 rearrangement	no FISH	46,XY,t(3;5)(q21;q31)[20]
54-BM	identified a TP53/IGL rearrangement	(TP53x3,D17Z1x2)[100/200]	54,XX,+1,del(4)(q21q27),+5,del(5)(q13q33)x2,+8,t(10;22)(p15;q11.2),+der(10)t(10;22),+11,+1 5,add(17)(p13),+18,+21[15]/46,XX[5]
78-BM	identified a cryptic MLLT10/KMT2A rearrangement in an apparently normal sample	(MLLT10x3,MLLx2)(MLLT10 con MLLx1)[462/500]	46,XX[20]

[a]Sample extracted from a fixed cell pellet.

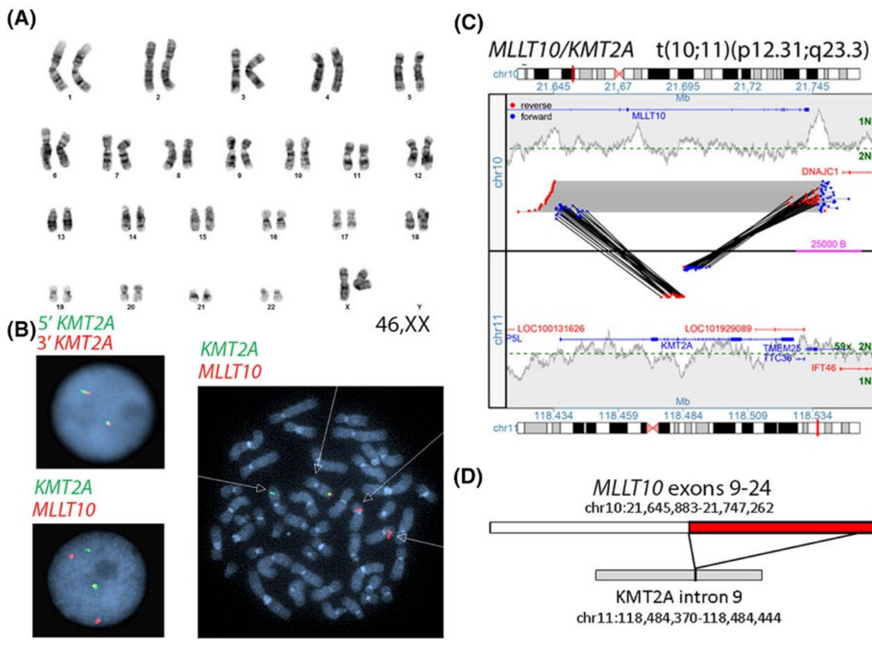

FIGURE 3 Sample 78-BM classified as a normal sample for this verification because we reported a normal karyotype shown in A and normal *KMT2A* break-apart FISH B, top figure. MPseq junction plot confirming an insertion of exons 9-24 of *MLLT10* (NM_004641) into intron 9 of *KMT2A* (NM_005933) in C and confirmed using an *MLLT10/KMT2A* D-FISH probe B, bottom figure

FGFR1/BCR fusion in a case with three *BCR* FISH signals. The identification of an *FGFR1* rearrangement provides further classification of this patient's AML in the WHO category of "Myeloid/lymphoid neoplasms with *FGFR1* rearrangements"[3] and could provide targeted therapeutic treatment options including FGFR inhibitors such as ponatinib.[13-17] In addition, MPseq identified a *MECOM/CDK6* fusion in AML case 46-PB with three *MECOM* FISH signals and a deletion 7q. *MECOM/CDK6* fusions have been described as recurrent "cryptic" abnormalities associated with increased *MECOM*/EVI expression and unfavorable prognosis.[18,19] Finally, while MPseq identified a *TP53/IGL* fusion in patient 54-BM with a RFR of rule out AML and with a FISH pattern indicating three *TP53* signals, the significance of this fusion is unknown. This patient (67 years old) is known to have AML with approximately 30%-40% blasts and a moderately hypercellular bone marrow (70%). The lymphocytes are not increased, they have unremarkable morphology and there is no evidence of lymphoma. To our knowledge, immunoglobulin translocations involving *TP53* have not been reported[20] in AML.

MPseq characterized the fusion partner of each of the four cases with a *NUP98* break-apart FISH result. Nucleoporin 98 (*NUP98*) located at 11p15 is a structural component of the nuclear pore complex and has been identified as a gene partner involved in numerous gene fusions.[21] *NUP98* rearrangements are most common in myeloid neoplasms, especially therapy-related AML, but can also be found in T-ALL.[21] AML patients with *NUP98* translocations are typically younger and have unfavorable prognosis compared to other AML subtypes.[22] Although the most common *NUP98* partner gene is *HOXA9*, in our validation cohort, we identified rarer fusions including *NUP98/SETBP1* (case 42-BM) in a young adult with AML, a *NUP98/PSIP1* (case 39-BM) in an adult with therapy-related AML[23] and *NUP98/KDM5A* (cases 40-BM and 41-BM) in two pediatric patients with acute megakaryoblastic leukemia (AMKL) representing a rare subtype of AML.[24-26] Since fusion of *NUP98* with *KDM5A* is a recurrent rearrangement in pediatric non-Down syndrome AMKL,[24-26] the MPseq result would have provided a specific, molecularly defined diagnosis with risk group stratification.

Importantly, a limitation of the MPseq assay is the inability to reliably detect clonal aberrations present at a very low level. MPseq cannot reliably detect structural rearrangements below 10%, while D-FISH strategies can detect specific rearrangements as low as 0.6%.[27] MPseq also cannot reliably detect copy number changes below 25%, while FISH can detect copy number changes as low as 1.5%-2.0% for homozygous deletions and trisomies and 4.5%-9.5% for heterozygous deletions and monosomies (data from our internal laboratory validation studies). In the accuracy cohort, MPseq was unable to reliably identify an apparent secondary trisomy 8 in three samples with abnormal FISH results at 2%, 3%, and 9%. Future improvements in the limit of detection of MPseq could be achieved by increasing the depth of sequencing and by improving the CNV detection algorithm. These limitations, however, are common to recently developed NGS-based technologies. A recent study by McKerrell et al[28] demonstrated an NGS-based tool for the diagnosis of myeloid malignancies; however, it was unable to detect some CNVs at 35% and was limited to detecting only four types of rearrangements. Another tool, Archer technology,[29,30] is also utilized for the detection of fusions common in AML but requires RNA for the detection of fusions, which is not an ideal specimen type compared to DNA since RNA is less stable and therefore requires additional measures taken by the laboratory to ensure RNA stability. Finally, the MPseq assay is not designed to detect point mutations; therefore, those subtypes of AML with recurrent genetic abnormalities based on genetic mutations, such as *CEBPA*, *FLT3* or *NPM1*, would not be detected by this MPseq assay.

In conclusion, we evaluated the performance of an NGS-based whole-genome MPseq technology with a targeted analysis approach to detect recurrent diagnostic and prognostic chromosomal rearrangements and copy number changes in patients with AML. We demonstrate the clinical utility of MPseq as a potential replacement assay for conventional FISH on diagnostic AML samples and highlight the resulting increased diagnostic yield and clarity in comparison to other testing methodologies (Table S4). MPseq provided important clinical value in cases in which there was a “cryptic” rearrangement not detected by FISH or chromosomes, or for those cases with additional uncharacterized FISH signals, or when a FISH break-apart result was identified without the availability of a reflex FISH probe to further define a suspected rearrangement. Due to the limitations in detecting very low-level abnormalities, MPseq would not be recommended for follow-up post therapy or minimal residual disease testing; utilization of FISH, RT-PCR or a custom fusion-qPCR strategy could be considered in those cases. It is important to note that the additional information identified in the MPseq data (Table 3) was filtered to reveal only the abnormalities on our predefined AML-panel filter. Future studies are underway to identify novel abnormalities throughout the genome associated with myeloid malignancies. As novel rearrangements and copy number alterations important in AML are uncovered in the future, the clinical MPseq panel can be easily expanded to include additional targets. The studies presented here demonstrate the value of MPseq as a novel NGS-based technology that has the potential to revolutionize the diagnosis of hematologic malignancies and provide an opportunity to advance precision medicine.

ACKNOWLEDGMENTS

We thank Saranya Sankaranarayanan, MS for bioinformatics help. This study was supported by development funds provided by the Department of Laboratory Medicine and Pathology, Mayo Clinic and partially funded by the Center for Individualized Medicine, Mayo Clinic.

CONFLICT OF INTEREST

Algorithms described in this manuscript are licensed to WholeGenome LLC owned by George Vasmatzis.

AUTHOR CONTRIBUTIONS

UA, SAS, BAP, KEP, ECT, RBJ, HMK, NLH, and LBB designed validation study; UA, SAS, BAP, and LBB wrote paper with help from SHJ, JBS, JFP, KBG, DLV, ECT, RBJ, RPK, PTG, HMK, and NLH; UA, SAS, BAP, ECT, RBJ, HMK, NLH, and LBB analyzed and interpreted data; RMZ, GV, SHJ, JBS, HMK, and NLH provided critical analytical tools; SAS and BAP collected data and PTG and RPK provided samples highlighted in manuscript.

ORCID

Umut Aypar http://orcid.org/0000-0002-2226-6163

REFERENCES

1. Grimwade D, Ivey A, Huntly BJ. Molecular landscape of acute myeloid leukemia in younger adults and its clinical relevance. *Blood*. 2016;127(1):29-41.
2. De Kouchkovsky I, Abdul-Hay M. Acute myeloid leukemia: a comprehensive review and 2016 update. *Blood Cancer J*. 2016;6(7):e441.
3. Arber DA, Orazi A, Hasserjian R, et al. The 2016 revision to the World Health Organization classification of myeloid neoplasms and acute leukemia. *Blood*. 2016;127(20):2391-2405.
4. Leonard JP, Martin P, Roboz GJ. Practical implications of the 2016 revision of the World Health Organization classification of lymphoid and myeloid neoplasms and acute leukemia. *J Clin Oncol*. 2017;35(23):2708-2715.
5. Aypar U, Knudson RA, Pearce KE, Wiktor AE, Ketterling RP. Development of an NPM1/MLF1 D-FISH probe set for the detection of t(3;5)(q25;q35) identified in patients with acute myeloid leukemia. *J Mol Diagn*. 2014;16(5):527-532.
6. Keefe JG, Sukov WR, Knudson RA, et al. Development of five dual-color, double-fusion fluorescence in situ hybridization assays for the detection of common MLL translocation partners. *J Mol Diagn*. 2010;12(4):441-452.
7. Johnson SH, Smadbeck JB, Smoley SA, et al. SVAtools for junction detection of genome-wide chromosomal rearrangements by mate-pair sequencing (MPseq). *Cancer Genet*. 2018;221:1-18.
8. Smadbeck JB, Johnson SH, Smoley SA, et al. Copy number variant analysis using genome-wide mate-pair sequencing. *Genes Chromosomes Cancer*. 2018;57:459-470.
9. Drucker TM, Johnson SH, Murphy SJ, Cradic KW, Therneau TM, Vasmatzis G. BIMA V3: an aligner customized for mate pair library sequencing. *Bioinformatics*. 2014;30(11):1627-1629.
10. Grimwade D, Hills RK, Moorman AV, et al. Refinement of cytogenetic classification in acute myeloid leukemia: determination of prognostic significance of rare recurring chromosomal abnormalities among 5876 younger adult patients treated in the United Kingdom Medical Research Council trials. *Blood*. 2010;116(3):354-365.
11. Harris NL, Jaffe ES, Diebold J, et al. World Health Organization classification of neoplastic diseases of the hematopoietic and lymphoid tissues: report of the Clinical Advisory Committee meeting-Airlie House, Virginia, November 1997. *J Clin Oncol*. 1999;17(12):3835-3849.
12. Dohner H, Estey E, Grimwade D, et al. Diagnosis and management of AML in adults: 2017 ELN recommendations from an international expert panel. *Blood*. 2017;129(4):424-447.
13. Demiroglu A, Steer EJ, Heath C, et al. The t(8;22) in chronic myeloid leukemia fuses BCR to FGFR1: transforming activity and specific inhibition of FGFR1 fusion proteins. *Blood*. 2001;98(13):3778-3783.
14. Fioretos T, Panagopoulos I, Lassen C, et al. Fusion of the BCR and the fibroblast growth factor receptor-1 (FGFR1) genes as a result of t(8;22)(p11;q11) in a myeloproliferative disorder: the first fusion gene involving BCR but not ABL. *Genes Chromosomes Cancer*. 2001;32(4):302-310.
15. Patterer V, Schnittger S, Kern W, Haferlach T, Haferlach C. Hematologic malignancies with PCM1-JAK2 gene fusion share characteristics with myeloid and lymphoid neoplasms with eosinophilia and abnormalities of PDGFRA, PDGFRB, and FGFR1. *Ann Hematol*. 2013;92(6):759-769.
16. Chase A, Bryant C, Score J, Cross NC. Ponatinib as targeted therapy for FGFR1 fusions associated with the 8p11 myeloproliferative syndrome. *Haematologica*. 2013;98(1):103-106.

17. Khodadoust MS, Luo B, Medeiros BC, et al. Clinical activity of ponatinib in a patient with FGFR1-rearranged mixed-phenotype acute leukemia. *Leukemia*. 2016;30(4):947-950.
18. Haferlach C, Bacher U, Grossmann V, et al. Three novel cytogenetically cryptic EVI1 rearrangements associated with increased EVI1 expression and poor prognosis identified in 27 acute myeloid leukemia cases. *Genes Chromosomes Cancer*. 2012;51(12):1079-1085.
19. Capela de Matos RR, Othman M, Ferreira GM, et al. Molecular approaches identify a cryptic MECOM rearrangement in a child with a rapidly progressive myeloid neoplasm. *Cancer Genet*. 2018;221:25-30.
20. Xu-Monette ZY, Medeiros LJ, Li Y, et al. Dysfunction of the TP53 tumor suppressor gene in lymphoid malignancies. *Blood*. 2012;119(16):3668-3683.
21. Gough SM, Slape CI, Aplan PD. NUP98 gene fusions and hematopoietic malignancies: common themes and new biologic insights. *Blood*. 2011;118(24):6247-6257.
22. Chou WC, Chen CY, Hou HA, et al. Acute myeloid leukemia bearing t(7;11)(p15;p15) is a distinct cytogenetic entity with poor outcome and a distinct mutation profile: comparative analysis of 493 adult patients. *Leukemia*. 2009;23(7):1303-1310.
23. Yamamoto K, Nakamachi Y, Yakushijin K, et al. Expression of the novel NUP98/PSIP1 fusion transcripts in myelodysplastic syndrome with t(9;11)(p22;p15). *Eur J Haematol*. 2012;88(3):244-248.
24. de Rooij JD, Branstetter C, Ma J, et al. Pediatric non-Down syndrome acute megakaryoblastic leukemia is characterized by distinct genomic subsets with varying outcomes. *Nat Genet*. 2017;49(3):451-456.
25. de Rooij JD, Hollink IH, Arentsen-Peters ST, et al. NUP98/JARID1A is a novel recurrent abnormality in pediatric acute megakaryoblastic leukemia with a distinct HOX gene expression pattern. *Leukemia*. 2013;27(12):2280-2288.
26. de Rooij JD, Masetti R, van den Heuvel-Eibrink MM, et al. Recurrent abnormalities can be used for risk group stratification in pediatric AMKL: a retrospective intergroup study. *Blood*. 2016;127(26):3424-3430.
27. Shearer BM, Sukov WR, Flynn HC, Knudson RA, Ketterling RP. Development of a dual-color, double fusion FISH assay to detect RPN1/EVI1 gene fusion associated with inv(3), t(3;3), and ins(3;3) in patients with myelodysplasia and acute myeloid leukemia. *Am J Hematol*. 2010;85(8):569-574.
28. McKerrell T, Moreno T, Ponstingl H, et al. Development and validation of a comprehensive genomic diagnostic tool for myeloid malignancies. *Blood*. 2016;128(1):e1–e9.
29. Zheng Z, Liebers M, Zhelyazkova B, et al. Anchored multiplex PCR for targeted next-generation sequencing. *Nat Med*. 2014;20(12):1479-1484.
30. Badar T, Johnson L, Trifilo K, et al. Detection of novel t(12;17)(p12;p13) in relapsed refractory acute myeloid leukemia by anchored multiplex PCR(AMP)-based next-generation sequencing. *Appl Immunohistochem Mol Morphol*. 2017.

SUPPORTING INFORMATION

Additional supporting information may be found online in the Supporting Information section at the end of the article.

How to cite this article: Aypar U, Smoley SA, Pitel BA, et al. Mate pair sequencing improves detection of genomic abnormalities in acute myeloid leukemia. *Eur J Haematol*. 2019;102:87–96. https://doi.org/10.1111/ejh.13179